Proton Shell Evolution below ^{132}Sn: First Measurement of Low-Lying β-Emitting Isomers in ^{123,125}Ag

Z. Q. Chen,[1] Z. H. Li,[1,*] H. Hua,[1,†] H. Watanabe,[2,3] C. X. Yuan,[4] S. Q. Zhang,[1] G. Lorusso,[3,5,6] S. Nishimura,[3] H. Baba,[3] F. Browne,[3,7] G. Benzoni,[8] K. Y. Chae,[9] F. C. L. Crespi,[8,10] P. Doornenbal,[3] N. Fukuda,[3] G. Gey,[3,11,12] R. Gernhäuser,[13] N. Inabe,[3] T. Isobe,[3] D. X. Jiang,[1] A. Jungclaus,[14] H. S. Jung,[15,16] Y. Jin,[1] D. Kameda,[3] G. D. Kim,[17] Y. K. Kim,[17,18] I. Kojouharov,[19] F. G. Kondev,[20] T. Kubo,[3] N. Kurz,[19] Y. K. Kwon,[17] X. Q. Li,[1] J. L. Lou,[1] G. J. Lane,[21] C. G. Li,[1] D. W. Luo,[1] A. Montaner-Pizá,[22] K. Moschner,[23] C. Y. Niu,[1] F. Naqvi,[24] M. Niikura,[25] H. Nishibata,[26] A. Odahara,[26] R. Orlandi,[27,28] Z. Patel,[6] Zs. Podolyák,[6] T. Sumikama,[3] P.-A. Söderström,[3] H. Sakurai,[3] H. Schaffner,[19] G. S. Simpson,[11] K. Steiger,[13] H. Suzuki,[3] J. Taprogge,[3,14,29] H. Takeda,[3] Zs. Vajta,[3,30] H. K. Wang,[31] J. Wu,[1,20] A. Wendt,[23] C. G. Wang,[1] H. Y. Wu,[1] X. Wang,[1] C. G. Wu,[1] C. Xu,[1] Z. Y. Xu,[25,32] A. Yagi,[26] Y. L. Ye,[1] and K. Yoshinaga[33]

[1]*School of Physics and State Key Laboratory of Nuclear Physics and Technology, Peking University, Beijing 100871, China*
[2]*IRCNPC, School of Physics and Nuclear Energy Engineering, Beihang University, Beijing 100191, China*
[3]*RIKEN Nishina Center, 2-1 Hirosawa, Wako, Saitama 351-0198, Japan*
[4]*Sino-French Institute of Nuclear Engineering and Technology, Sun Yat-Sen University, Zhuhai, 519082, Guangdong, China*
[5]*National Physical Laboratory, NPL, Teddington, Middlesex TW11 0LW, United Kingdom*
[6]*Department of Physics, University of Surrey, Guildford GU2 7XH, United Kingdom*
[7]*School of Computing, Engineering and Mathematics, University of Brighton, Brighton, BN2 4GJ, United Kingdom*
[8]*INFN, Sezione di Milano, via Celoria 16, I-20133 Milano, Italy*
[9]*Department of Physics, Sungkyunkwan University, Suwon 440-746, Republic of Korea*
[10]*Dipartimento di Fisica, Universitá di Milano, via Celoria 16, I-20133 Milano, Italy*
[11]*LPSC, Universite Joseph Fourier Grenoble 1, CNRS/IN2P3, Institut National Polytechnique de Grenoble, F-38026 Grenoble Cedex, France*
[12]*Institut Laue-Langevin, B.P. 156, F-38042 Grenoble Cedex 9, France*
[13]*Physik Department, Technische Universität München, D-85748 Garching, Germany*
[14]*Instituto de Estructura de la Materia, CSIC, E-28006 Madrid, Spain*
[15]*Department of Physics, Chung-Ang University, Seoul 156-756, Republic of Korea*
[16]*Department of Physics, University of Notre Dame, Notre Dame, Indiana 46556, USA*
[17]*Rare Isotope Science Project, Institute for Basic Science, Daejeon 305-811, Republic of Korea*
[18]*Department of Nuclear Engineering, Hanyang University, Seoul 133-791, Republic of Korea*
[19]*GSI Helmholtzzentrum für Schwerionenforschung GmbH, 64291 Darmstadt, Germany*
[20]*Physics Division, Argonne National Laboratory, Lemont, Illinois 60439, USA*
[21]*Department of Nuclear Physics, R.S.P.E., Australian National University, Canberra, Australian Capital Territory 0200, Australia*
[22]*IFIC, CSIC-Universidad de Valencia, A.C. 22085, E 46071, Valencia, Spain*
[23]*Institut für Kernphysik, Universität zu Köln, Zülpicher Strasse 77, D-50937 Köln, Germany*
[24]*Wright Nuclear Structure Laboratory, Yale University, New Haven, Connecticut 06520-8120, USA*
[25]*Department of Physics, University of Tokyo, Hongo 7-3-1, Bunkyo-ku, 113-0033 Tokyo, Japan*
[26]*Department of Physics, Osaka University, Machikaneyama-machi 1-1, Osaka 560-0043 Toyonaka, Japan*
[27]*Instituut voor Kern en Stralingsfysica, KU Leuven, University of Leuven, B-3001 Leuven, Belgium*
[28]*Advanced Science Research Center, Japan Atomic Energy Agency, Tokai, Ibaraki, 319-1195, Japan*
[29]*Departamento de Física Teórica, Universidad Autónoma de Madrid, E-28049 Madrid, Spain*
[30]*MTA Atomki, P.O. Box 51, Debrecen, H-4001, Hungary*
[31]*College of Physics and Telecommunication Engineering, Zhoukou Normal University, Henan 466000, People's Republic of China*
[32]*Department of Physics, the University of Hong Kong, Pokfulam Road, Hong Kong*
[33]*Department of Physics, Faculty of Science and Technology, Tokyo University of Science, 2641 Yamazaki, Noda, Chiba, Japan*

(Received 3 February 2019; revised manuscript received 1 April 2019; published 28 May 2019)

The β-delayed γ-ray spectroscopy of neutron-rich ^{123,125}Ag isotopes is investigated at the Radioactive Isotope Beam Factory of RIKEN, and the long-predicted $1/2^-$ β-emitting isomers in ^{123,125}Ag are identified for the first time. With the new experimental results, the systematic trend of energy spacing between the lowest $9/2^+$ and $1/2^-$ levels is extended in Ag isotopes up to $N = 78$, providing a clear signal for the reduction of the $Z = 40$ subshell gap in Ag towards $N = 82$. Shell-model calculations with the state-of-the-art V_{MU} plus M3Y spin-orbit interaction give a satisfactory description of the low-lying states in ^{123,125}Ag.

The tensor force is found to play a crucial role in the evolution of the size of the $Z = 40$ subshell gap. The observed inversion of the single-particle levels around ^{123}Ag can be well interpreted in terms of the monopole shift of the $\pi 1g_{9/2}$ orbitals mainly caused by the increasing occupation of $\nu 1h_{11/2}$ orbitals.

DOI: 10.1103/PhysRevLett.122.212502

With nuclear physics studies moving towards radioactive nuclei far from the β-stability line over the past decades, the well-known magic nucleon numbers (8, 20, 28, 50, 82, and 126) were found to be not necessarily immutable across the nuclear chart [1,2]. To investigate the underlying mechanism which alters the magic numbers, considerable experimental and theoretical efforts have been made. Nowadays, the evolution of shell structure is known to be largely affected by the strong nucleon-nucleon tensor interaction [3–6].

In recent years, much attention has been focused on the detailed location and magnitude of shell and subshell gaps in different mass regions [1,6–10]. One of the regions of particular interest lies below the doubly magic nucleus ^{132}Sn. A quenching of the $N = 82$ shell gap was predicted a long time ago [11–13] to take place below ^{132}Sn. Because of experimental difficulties to produce these extremely neutron-rich nuclides, so far only a few nuclides below $Z = 50$ have been studied around $N = 82$. Recent experimental studies have shown that the $N = 82$ shell closure in ^{132}Sn, ^{130}Cd, and ^{128}Pd isotones is still robust [14–18], but a significant reduction of the $N = 82$ gap was suggested to occur between Sn and Zr as a consequence of the absent $Z = 40$ subshell gap [7]. Therefore, when moving away from $Z = 50$, it is very important to further investigate where the predicted quenching of the $N = 82$ shell gap and the $Z = 40$ subshell gap [7,19] will occur, as well as how the neutron shell gap and proton subshell gap influence each other. In addition, nuclei close to ^{132}Sn and their structure properties are relevant for the astrophysical rapid neutron-capture process, the r process [20,21]. A good understanding of the $N = 82$ magic shell and its evolution along the r-process path is of crucial importance for the nucleosynthesis calculations in this region [20].

Owing to recent developments in producing intense rare isotope beams worldwide in combination with efficient particle and γ-ray detection systems, it has become possible to make detailed spectroscopic studies of neutron-rich nuclei below ^{132}Sn. With the $Z = 47$, the neutron-rich odd-A Ag isotopes are naturally of great interest. Their valence protons are assumed to fill the $\pi 1g_{9/2}$ and $\pi 2p_{1/2}$ orbitals, between which the $Z = 40$ subshell gap is formed. Consequently, the energy difference between the lowest-lying $9/2^+$ and $1/2^-$ states in these neutron-rich odd-A Ag isotopes provides direct information on the $Z = 40$ subshell gap.

To illustrate how the $Z = 40$ subshell gap evolves in Ag isotopes, the energy differences between the lowest $9/2^+$ and $1/2^-$ states are summarized for odd-A silver isotopes with $N = 48$–78 in Fig. 1. On the neutron-deficient side, the systematic trend of the energy spacing, as well as theoretical calculations [22,23], suggests a maximum at $N = 50$, manifesting the stability of both $Z = 40$ and $N = 50$ shell gaps in Ag isotopes. With the increase of the neutron number, this energy difference drops quickly. At ^{105}Ag ($N = 58$), the ordering of these two levels swaps and the $1/2^-$ state becomes the lowest state. The energy splittings between the lowest $9/2^+$ and $1/2^-$ states are relatively flat in the neutron midshell region till ^{119}Ag ($N = 72$), where the $1/2^-$ isomeric state was proposed to lie between the $7/2^+$ ground state and the $9/2^+$ excited state at 130 keV [24,25]. For nuclei beyond ^{119}Ag, so far only the $9/2^+$ states are assigned in ^{121,123,125}Ag mainly based on the systematics [26–30], while no experimental information on $1/2^-$ states is available. Therefore, it is very interesting to see how the $1/2^-$ state will evolve with respect to the $9/2^+$ state in the heavier Ag isotopes when approaching $N = 82$: Will it remain below the $9/2^+$ state or get even lower, or will the order of the states change?

In this Letter, we report on spectroscopic studies of neutron-rich odd-A Ag isotopes via β decay of Pd isotopes. The aim of the present study is to determine the positions of the $2p_{1/2}$ proton-hole states in neutron-rich ^{123,125}Ag isotopes.

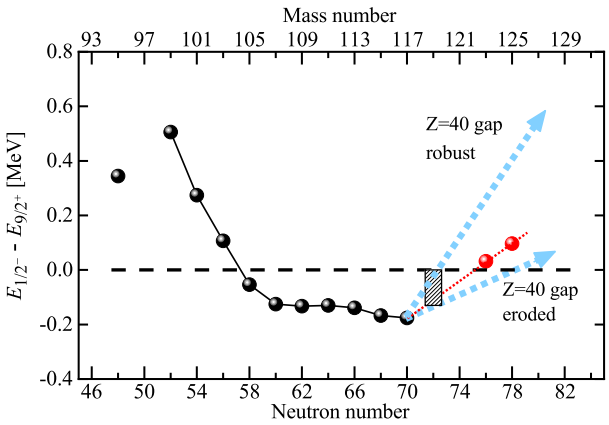

FIG. 1. Systematics of experimental energy differences between the lowest-lying $1/2^-$ and $9/2^+$ states in Ag isotopes. Data are taken from Refs. [24,31] (black filled circles) and the present work (red filled circles). The dashed blue arrows are drawn to guide the eye. The range of the shaded region for ^{119}Ag corresponds to the uncertainties of the experimental data.

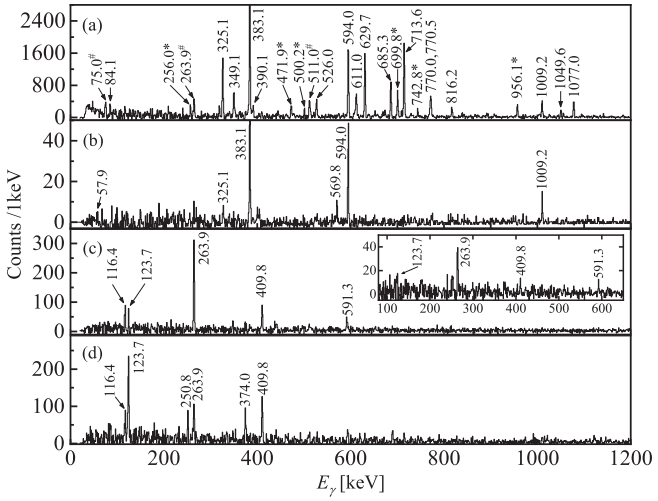

FIG. 2. (a) β-delayed γ-ray spectra measured within 300 ms after the ^{123}Pd implantation. The peaks marked with asterisks are new transitions in ^{123}Ag but not included in the partial level scheme in Fig. 4, and the peaks marked with # are known contaminants. (b) Coincident γ-ray spectra gated on the 611.0-keV γ ray. The γ-ray spectra in β-delayed coincidence with the sum of (c) the 713.6-, 629.7-, and 685.3-keV transitions and (d) 383.1-, 325.1-, and 594.0-keV transitions. Inset in (c): The γ-ray spectrum in β-delayed coincidence with the 1009.2-keV transition.

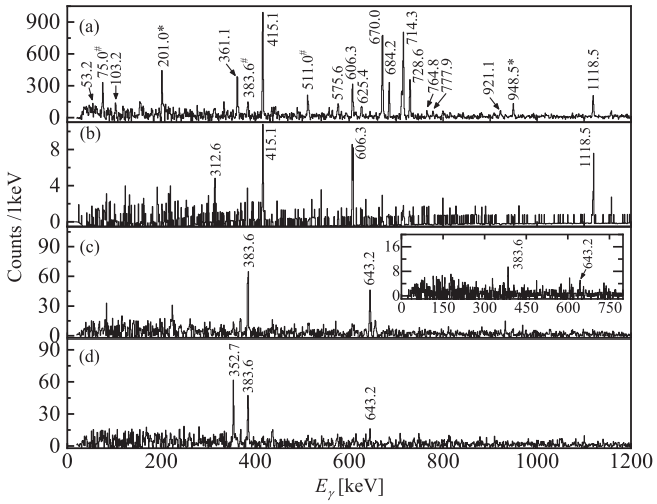

FIG. 3. (a) β-delayed γ-ray spectra measured within 180 ms after the ^{125}Pd implantation. The peaks marked with asterisks are new transitions in ^{125}Ag but not included in the partial level scheme in Fig. 4, and the peaks marked with # are known contaminants. (b) Coincident γ-ray spectra gated on the 625.4-keV γ ray. The γ-ray spectra in β-delayed coincidence with the sum of (c) the 714.3-, 670.0-, and 728.6-keV transitions and (d) 415.1-, 361.1-, and 606.3-keV transitions. Inset in (c): The γ-ray spectrum in β-delayed coincidence with the 1118.5-keV transition.

The experiment was performed at the Radioactive Isotope Beam Factory (RIBF) facility [32] at RIKEN in the framework of the Euroball RIken Cluster Array (EURICA) project [33,34]. A primary beam of 345 MeV/u ^{238}U^{86+}, with an intensity of 7–12 pnA, impinged into a 3-mm-thick Be target. The ions of interest were separated and identified event by event by the BigRIPS and ZeroDegree spectrometers [35]. A total of about 7.0×10^6 ^{123}Pd^{46+} and 2.4×10^6 ^{125}Pd^{46+} ions were implanted into an active stopper, named WAS3ABi [33], which consisted of eight compactly stacked double-sided silicon-strip detectors (DSSSDs). The WAS3ABi array also served as a detector for the beta particles (electrons). Gamma rays emitted after the β decays of the implanted ions were detected with the EURICA spectrometer [34], which consisted of 84 high-purity germanium crystals grouped in 12 clusters.

The ground state of ^{123}Ag has been assigned as $7/2^+$ based on the systematics and its decay pattern [27–29]. A low-lying $9/2^+$ level only 27 keV above the $7/2^+$ ground state has been reported in ^{123}Ag [27,28]. The ground state of ^{125}Ag was assigned as $9/2^+$ based on the similar γ-decay pattern as ^{123}Ag and on the systematics [27,28]. In the previous studies [27,28], a short-lived (submicrosecond) $17/2^-$ isomeric state was observed in both ^{123}Ag and ^{125}Ag, and their γ-decay schemes were established. In the present work, most of the previously reported γ transitions following the $17/2^-$ isomeric decay in ^{123}Ag and ^{125}Ag can be clearly seen in the β-delayed γ-ray spectra of corresponding Pd isotopes, as shown in Figs. 2(a) and 3(a). Besides, many new γ rays are observed.

The partial level schemes of ^{123}Ag and ^{125}Ag deduced from the present work are shown in Fig. 4. It can be seen that these two isotopes have a similar decay pattern. Figures 2(b) and 3(b) present examples of coincidence spectra in ^{123}Ag and ^{125}Ag, respectively. For ^{123}Ag, the 611.0-keV transition has a clear coincidence with the 1009.2-keV transition, as well as with the 383.1- and 594.0-keV transitions. Meanwhile, the 383.1- and 594.0-keV transitions are found to be in coincidence with each other but not with the 1009.2-keV transition. The coincidence pattern suggests that the 611.0-keV transition feeds a level, which decays via two parallel transition paths. One deexcites via the 1009.2-keV transition, and the other decays via a transition sequence of 383.1 and 594.0 keV.

For ^{125}Ag, the 625.4-keV transition has a clear coincidence with the 1118.5-keV transition, as well as with the 415.1- and 606.3-keV transitions [see Fig. 3(b)]. The 415.1- and 606.3-keV transitions are found to be in coincidence with each other but not with the 1118.5-keV transition. Based on the γ-γ coincidence, intensity balance, and systematics of the odd-A Ag isotopes, for ^{125}Ag, the transition sequence of 415.1 and 606.3-keV is suggested to deexcite to the $1/2^-$ long-predicted isomeric state, and the 1118.5-keV transition decays to the $9/2^+$ ground state. The remarkable similarity of γ-γ coincidence of ^{123,125}Ag

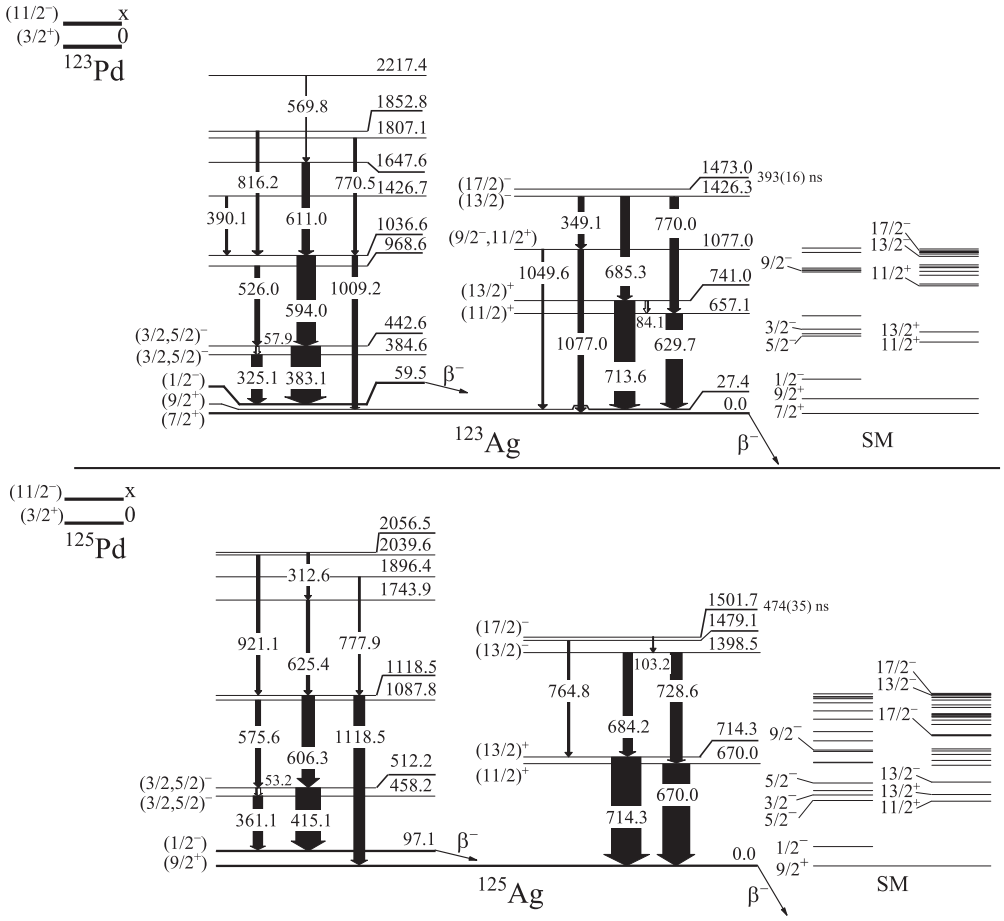

FIG. 4. Partial level schemes of ^{123}Ag and ^{125}Ag constructed in this work in comparison with the shell-model calculations. The experimental information of $17/2^-$ isomeric states in ^{123,125}Ag, which are not or weakly populated in the present work due to the selection rule, are taken from Ref. [27]. The arrow widths are proportional to their absolute intensities.

suggests that, for ^{123}Ag, the transition sequence of 383.1 and 594.0-keV feeds the $1/2^-$ isomeric state, and the 1009.2-keV transition decays to the $9/2^+$ state.

The $1/2^-$ states in ^{123,125}Ag are predicted to be β-decaying isomers. To further explore their decays to Cd isotopes, an asymmetric matrix with γ rays from the daughter Ag nuclei on one axis and γ rays from the granddaughter Cd nuclei on the other axis was constructed. To get clean coincident γ-ray spectra, the time ranges of γ rays from mother nuclei decay and daughter nuclei decay are set as twice the half-life for each of the respective nuclei. Figures 2(c)–2(d) and Figures 3(c)–3(d) exhibit the γ-ray spectra of the granddaughter nuclei ^{123}Cd and ^{125}Cd with gates on the γ rays of the daughter nuclei ^{123}Ag and ^{125}Ag, respectively. As illustrated in Fig. 2(c), with gates on the known 713.6-, 629.7-, and 685.3-keV γ transitions which finally feed the $7/2^+$ ground state of ^{123}Ag, a strong 263.9-keV γ ray and several relative weak 116.4-, 123.7-, 409.8-, and 591.3-keV γ rays can be clearly seen. In contrast, with gates on the γ rays at energies of 325.1, 383.1, and 594.0 keV which finally feed the $1/2^-$ isomeric state of ^{123}Ag, the 123.7-keV transition becomes the strongest [although the 263.9-keV γ ray can also been seen in Fig. 2(d)]. Furthermore, the resulting γ-ray spectrum of granddaughter ^{123}Cd with a gate on the 1009.2-keV transition in ^{123}Ag shown in the inset in Fig. 2(c) is very similar to Fig. 2(c) rather than Fig. 2(d). Such different populating patterns in granddaughter ^{123}Cd reveal that these two groups of γ-ray transitions (i.e., the 713.6-, 629.7-, 685.3-, and 1009.2-keV transitions and 325.1-, 383.1-, and 594.0-keV transitions) finally feed the different β-decaying states in ^{123}Ag, which firmly verify the identification of the $1/2^-$ isomeric state in ^{123}Ag in the present work. As shown in Figs. 3(c) and 3(d), the different populating patterns can also be seen in ^{125}Cd.

To further probe the nature of the low-lying states in ^{123}Ag and ^{125}Ag, shell-model calculations have been performed using the KSHELL code [36] with the state-of-the-art monopole-based universal interaction V_{MU} plus a spin-orbit force from M3Y(V_{MU} + LS) [4,37]. The V_{MU} interaction consists of a Gaussian central force and a tensor force [4] and has successfully been applied to describe the shell structure of exotic nuclei in many regions [5,38–41]. In the present calculations, the model space consists of four proton orbitals ($1f_{5/2}$, $2p_{3/2}$, $2p_{1/2}$, and $1g_{9/2}$) and five

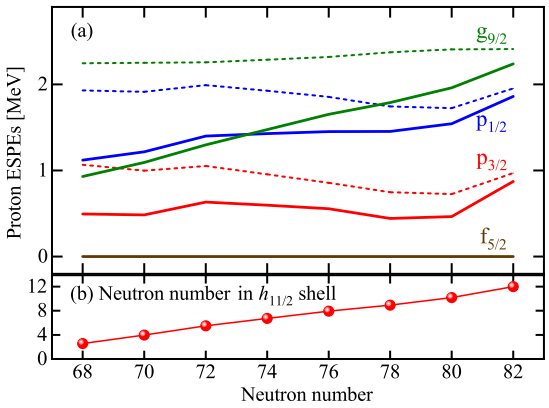

FIG. 5. (a) Proton effective single-particle energies in Ag isotopes calculated by the $V_{\mathrm{MU}}+\mathrm{LS}$ interaction. The dashed lines are obtained only with the central and spin-orbit forces, while the solid lines include the central, spin-orbit, and tensor forces. (b) Neutron occupation number in the $1h_{11/2}$ shell.

neutron orbitals ($1g_{7/2}$, $2d_{5/2}$, $3s_{1/2}$, $1h_{11/2}$, and $2d_{3/2}$) with ^{78}Ni as an inert core. Since the deeply bound proton orbitals ($1f_{5/2}$ and $2p_{3/2}$) and neutron orbitals ($1g_{7/2}$ and $2d_{5/2}$) are not expected to play major roles in the low-lying states in Ag isotopes, these orbitals are fully occupied. The calculated levels are plotted in Fig. 4 in comparison with the experimental results. It can be seen that shell-model calculations give an overall satisfactory description of experimental levels in ^{123,125}Ag, particularly for the low-lying levels. The calculations indicate that, as approaching $N=82$, the wave functions from the $\pi 1g_{9/2}$ and $\pi 2p_{1/2}$ orbitals dominate low-lying states of Ag isotopes.

With the newly observed $1/2^-$ isomeric states in ^{123,125}Ag, Fig. 1 shows that the $9/2^+$ and $1/2^-$ levels swap their ordering again around ^{123}Ag. The systematic energy difference indicates an increasing trend beyond ^{125}Ag, which reveals that the $Z=40$ subshell gap formed between the $\pi 1g_{9/2}$ and $\pi 2p_{1/2}$ orbitals starts to be restored toward $N=82$. It is worth emphasizing that, although the energy difference between the $9/2^+$ and $1/2^-$ levels shows a similar trend toward $N=82$ as that toward $N=50$, the slope at the neutron-rich side is obviously much less steep than on the neutron-deficient side close to $N=50$. Extrapolating the trend toward $N=82$, a considerable diminishment of the $Z=40$ subshell gap is expected.

To get more insight into the microscopic origin of shell evolution in this region, the effective single-particle energies (ESPEs) are calculated for the proton orbitals in the region of $N=68$–82 with the $V_{\mathrm{MU}}+\mathrm{LS}$ interaction and shown in Fig. 5(a). Here, the V_{MU} interaction is decomposed into the two components, i.e., the central and tensor parts, to identify their possible effects on the shell evolution. To show the influence from the neutron $\nu 1h_{11/2}$ orbital in the proton-neutron tensor force, the calculated neutron occupation number in the $1h_{11/2}$ shell is presented in Fig. 5(b). It can be seen that, if only the central + spin-orbit parts are considered, the $\pi 2p_{1/2}$ orbital lies below the $\pi 1g_{9/2}$ orbital in the whole region of $N=68$–82 [see dashed lines in Fig. 5(a)]. In contrast, with the inclusion of the tensor part (especially the $\pi 1g_{9/2}$-$\nu 1h_{11/2}$ monopole), the $\pi 1g_{9/2}$ orbital is affected much more than the $\pi 2p_{1/2}$ orbital, and the spacing between $\pi 1g_{9/2}$ and $\pi 2p_{1/2}$ orbitals is notably reduced [see solid lines in Fig. 5(a)], consequently, results in the inversion of these two orbitals at $N\sim 74$, which is compatible with the experimental inversion position. In view of this picture, the tensor force manifests its crucial role in the modification of the order of the proton orbitals and the size of the $Z=40$ subshell gap in Ag isotopes mainly through the $\pi 1g_{9/2}$-$\nu 1h_{11/2}$ monopole. Vice versa, our calculations indicate that this tensor force will also influence the behavior of the $\nu 1h_{11/2}$ orbital, which is important for the $N=82$ shell gap.

In conclusion, spectroscopic studies of neutron-rich ^{123,125}Ag have been performed via the β decays of ^{123,125}Pd at RIKEN, and the long-predicted $1/2^-$ isomeric states in ^{123,125}Ag have been successfully identified for the first time. The systematic trend of the energy spacing between the lowest-lying $9/2^+$ and $1/2^-$ levels in the Ag isotopes provides a clear signal of a reduction of the $Z=40$ subshell as approaching $N=82$. Shell-model calculations with the $V_{\mathrm{MU}}+\mathrm{LS}$ interaction reproduce well the experimental low-lying states in ^{123,125}Ag. The tensor force is found to play a crucial role in the evolution of the size of the $Z=40$ subshell gap.

This work was carried out at the RIBF operated by RIKEN Nishina Center, RIKEN and CNS, University of Tokyo. We thank the staff at RIBF for providing the beams, the EUROBALL Owners Committee for the loan of germanium detectors, and the PreSpec Collaboration for the use of the readout electronics. Part of the WAS3ABi was supported by the Rare Isotope Science Project which is funded by MSIP and NRF of Korea. This work was supported by the National Key R&D Program of China (Contract No. 2018YFA0404403), the Natural Science Foundation of China under Grants No. 11775003, No. 11675003, No. 11775316, and No. 11875075, the National Research Foundation of Korea (No. NRF-2016R1A5A1013277 and No. NRF-2013M7A1A1075764), and the Spanish Ministerio de Economía y Competitividad under Contract No. FPA2017-84756-C4-2-P. This work was partially supported by JSPS KAKENHI (Grants No. 25247045 and No. 17H06090). Work at ANL is supported by the U.S. Department of Energy, Office of Science, Office of Nuclear Physics, under Contract No. DE-AC02-06CH11357.

*zhli@pku.edu.cn
†hhua@pku.edu.cn

[1] O. Sorlin and M.-G. Porquet, Prog. Part. Nucl. Phys. **61**, 602 (2008).

[2] D. Steppenbeck *et al.*, Nature (London) **502**, 207 (2013).
[3] T. Otsuka, T. Suzuki, R. Fujimoto, H. Grawe, and Y. Akaishi, Phys. Rev. Lett. **95**, 232502 (2005).
[4] T. Otsuka, T. Suzuki, M. Honma, Y. Utsuno, N. Tsunoda, K. Tsukiyama, and M. Hjorth-Jensen, Phys. Rev. Lett. **104**, 012501 (2010).
[5] T. Otsuka, Phys. Scr. **T152**, 014007 (2013).
[6] H. Watanabe *et al.*, Phys. Rev. Lett. **113**, 042502 (2014).
[7] J. Taprogge *et al.*, Phys. Rev. Lett. **112**, 132501 (2014).
[8] E. Sahin *et al.*, Phys. Rev. Lett. **118**, 242502 (2017).
[9] L. Olivier *et al.*, Phys. Rev. Lett. **119**, 192501 (2017).
[10] D. Steppenbeck *et al.*, Phys. Rev. Lett. **114**, 252501 (2015).
[11] J. Dobaczewski, I. Hamamoto, W. Nazarewicz, and J. A. Sheikh, Phys. Rev. Lett. **72**, 981 (1994).
[12] J. Dobaczewski, W. Nazarewicz, and T. R. Werner, Phys. Scr. **T56**, 15 (1995).
[13] J. Dobaczewski, W. Nazarewicz, T. Werner, J. Berger, C. Chinn, and J. Dechargé, Phys. Rev. C **53**, 2809 (1996).
[14] A. Jungclaus *et al.*, Phys. Rev. Lett. **99**, 132501 (2007).
[15] M. Dworschak *et al.*, Phys. Rev. Lett. **100**, 072501 (2008).
[16] K. L. Jones *et al.*, Nature (London) **465**, 454 (2010).
[17] H. Watanabe *et al.*, Phys. Rev. Lett. **111**, 152501 (2013).
[18] J. M. Allmond *et al.*, Phys. Rev. Lett. **112**, 172701 (2014).
[19] H.-K. Wang, K. Kaneko, and Y. Sun, Phys. Rev. C **91**, 021303(R) (2015).
[20] K.-L. Kratz, B. Pfeiffer, O. Arndt, S. Hennrich, and A. Wöhr, Eur. Phys. J. A **25**, 633 (2005).
[21] M. Mumpower, R. Surman, G. McLaughlin, and A. Aprahamian, Prog. Part. Nucl. Phys. **86**, 86 (2016).
[22] K. Schmidt *et al.*, Nucl. Phys. **A624**, 185 (1997).
[23] L. Coraggio, A. Covello, A. Gargano, N. Itaco, and T. T. S. Kuo, J. Phys. G **26**, 1697 (2000).
[24] http://www.nndc.bnl.gov/ensdf/.
[25] H. Penttilä, J. Äystö, K. Eskola, Z. Janas, P. P. Jauho, A. Jokinen, M. E. Leino, J. M. Parmonen, and P. Taskinen, Z. Phys. A **338**, 291 (1991).
[26] Y. Kim, S. Biswas, M. Rejmund, A. Navin, A. Lemasson, S. Bhattacharyya, M. Caamao, E. Clment, G. de France, and B. Jacquot, Phys. Lett. B **772**, 403 (2017).
[27] S. Lalkovski *et al.*, Phys. Rev. C **87**, 034308 (2013).
[28] I. Stefanescu *et al.*, Eur. Phys. J. A **42**, 407 (2009).
[29] S. Ohya, Nucl. Data Sheets **102**, 547 (2004).
[30] http://www.nndc.bnl.gov.
[31] J. K. Hwang *et al.*, Phys. Rev. C **65**, 054314 (2002).
[32] Y. Yano, Nucl. Instrum. Methods Phys. Res., Sect. B **261**, 1009 (2007).
[33] S. Nishimura, Prog. Theor. Exp. Phys. **2012**, 03C006 (2012).
[34] P.-A. Söderström *et al.*, Nucl. Instrum. Methods Phys. Res., Sect. B **317**, 649 (2013).
[35] T. Kubo, Nucl. Instrum. Methods Phys. Res., Sect. B **204**, 97 (2003).
[36] N. Shimizu, arXiv:1310.5431v1.
[37] G. Bertsch, J. Borysowicz, H. McManus, and W. G. Love, Nucl. Phys. **A284**, 399 (1977).
[38] T. Otsuka, A. Gade, O. Sorlin, T. Suzuki, and Y. Utsuno, arXiv:1805.06501v3.
[39] T. Togashi, N. Shimizu, Y. Utsuno, T. Otsuka, and M. Honma, Phys. Rev. C **91**, 024320 (2015).
[40] C. X. Yuan *et al.*, Phys. Lett. B **762**, 237 (2016).
[41] M. Queiser *et al.*, Phys. Rev. C **96**, 044313 (2017).